

Fully Automatic, Semiautomatic, and Manual Corneal Nerve Fiber Analysis in Patients With Sarcoidosis

Lisette R. M. Raasing¹, Oscar J. M. Vogels², Mirjam Datema³, Martijn R. Tannemaat⁴, Marcel Veltkamp^{1,5}, and Jan C. Grutters^{1,5}

¹ ILD Center of Excellence, Department of Pulmonology, St. Antonius Hospital, Nieuwegein, the Netherlands

² ILD Center of Excellence, Department of Neurology, St. Antonius Hospital, Nieuwegein, the Netherlands

³ Department of Clinical Neurophysiology, St. Antonius Hospital, Nieuwegein, the Netherlands

⁴ Department of Clinical Neurophysiology, Leiden University Medical Center, Leiden, the Netherlands

⁵ Division of Heart and Lungs, University Medical Center Utrecht, Utrecht, the Netherlands

Correspondence: Lisette R. M. Raasing, ILD Center of Excellence, Department of Pulmonology, St. Antonius Hospital, 3435 CM, Nieuwegein, the Netherlands. e-mail: l.raasing@antoniusziekenhuis.nl

Received: April 11, 2023

Accepted: November 3, 2023

Published: December 4, 2023

Keywords: corneal confocal microscopy; sarcoidosis; image analysis; nerve fiber area; nerve fiber length

Citation: Raasing LRM, Vogels OJM, Datema M, Tannemaat MR, Veltkamp M, Grutters JC. Fully automatic, semiautomatic, and manual corneal nerve fiber analysis in patients with sarcoidosis. *Transl Vis Sci Technol.* 2023;12(12):3. <https://doi.org/10.1167/tvst.12.12.3>

Purpose: No guidelines are available on the preferred method for analyzing corneal confocal microscopy (CCM) data. Manual, semiautomatic, and automatic analyzes are all currently in use. The purpose of the present study was threefold. First, we aimed to investigate the different methods for CCM analysis in patients with and without small fiber neuropathy (SFN). Second, to determine the correlation of different methods for measuring corneal nerve fiber length (CNFL) and nerve fiber area (NFA). Finally, we investigated the added value of automatic NFA analysis.

Methods: We included 20 healthy controls and 80 patients with sarcoidosis, 31 with established SFN and 49 without SFN. The CNFL was measured using CCMetrics, ACCMetrics, and NeuronJ. NFA was measured with NFA FIJI and ACCMetrics NFA.

Results: CNFL and NFA could not distinguish sarcoidosis with and without SFN or healthy controls. CCMetrics, NeuronJ, and ACCMetrics CNFL highly correlated. Also, NFA FIJI and ACCMetrics NFA highly correlated. Reproducing a nonlinear formula between CNFL and NFA confirmed the quadratic relation between NFA FIJI and ACCMetrics CNFL. CCMetrics and NeuronJ instead showed a square root relationship and seem to be less comparable owing to differences between automatic and manual techniques.

Conclusions: ACCMetrics can be used for fully automatic analysis of CCM images to optimize efficiency. However, CNFL and NFA do not seem to have a discriminatory value for SFN in sarcoidosis. Further research is needed to determine the added value and normative values of NFA in CCM analysis.

Translational Relevance: Our study improves the knowledge about CCM software and pathophysiology of SFN.

Introduction

Sarcoidosis is a systemic inflammatory disease of unknown cause, primarily affecting intrathoracic lymph nodes, lungs, and skin.¹ Small fiber neuropathy (SFN) is the result of damaged small myelinated (A δ -fibers) and unmyelinated (C-fibers) nerve fibers. It is estimated that between 40% and 86% of patients with sarcoidosis suffer from SFN related symptoms.^{2,3} There is no gold standard available for the diagnosis of

SFN, but the Neurodiab criteria⁴ are currently the best described criteria. These criteria are based on a large group of patients with diabetes and define three levels of diagnostic certainty.

For a diagnosis of possible SFN, symptoms and/or signs of neuropathic sensory symptoms should be present. A diagnosis of probable SFN additionally includes normal nerve conduction studies. To diagnose definite SFN, reduced intraepidermal nerve fiber density and/or abnormal quantitative sensory testing (QST) is also required.⁴ A more recent reappraisal and

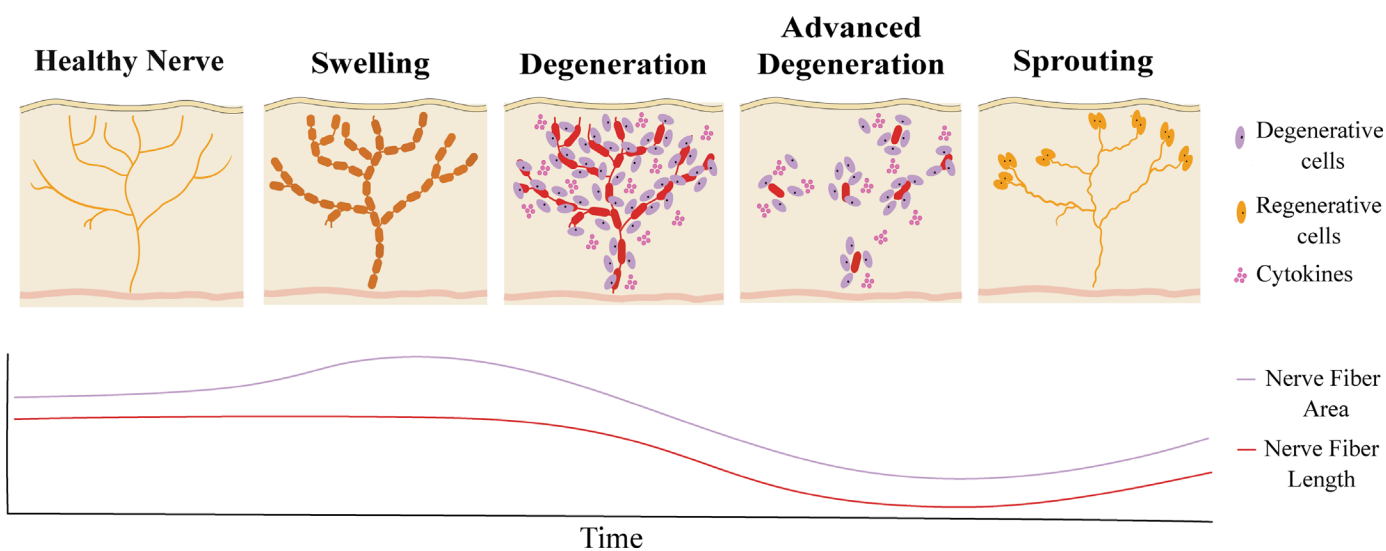


Figure 1. Schematic presentation of a small nerve fiber in different stages in the epidermis. A healthy nerve has a small diameter. The small nerve swells at an early pathological stage before degenerating and can be recognized as SFN with reduced nerve fiber density. Advanced degeneration results severely reduced intraepidermal nerve fiber density. After degeneration, sprouting results in new nerve structures. The graph below shows a schematic progression of NFA and CNFL during the stages of healthy nerve, nerve swelling and nerve degeneration. NFA can detect nerve swelling in the early stage of SFN by measuring an increasing number of pixels in the nerve structures. CNFL will measure a reduced number of pixels when nerve degeneration appears.

validation study increased the reliability of the diagnosis by stating that at least two clinical signs should be present.⁵

A very complex and time-consuming protocol has been proposed to determine the intraepidermal nerve fiber density.^{6,7} QST shows varying reliability owing to the lack of standardized data.⁸ Therefore, corneal confocal microscopy (CCM) has been investigated to detect SFN as a novel and minimally invasive alternative.^{9,10} CCM generates *in vivo* images of the corneal sub-basal nerve plexus with resolutions comparable with *ex vivo* histochemical methods.¹¹

Although research has been conducted over the past 20 years to support its clinical use, CCM is still used primarily for research purposes only. Many hurdles have already been overcome in translating this technique from research to clinical use. For example, normative values are available¹² and a detailed protocol can be used for the accurate quantification of peripheral neuropathy.¹³ In addition, a solid body of literature is currently available to support the usefulness of CCM in neurodegenerative diseases.¹⁴

The cornea harbors a high nerve fiber density, up to 400 times higher compared with intraepidermal nerve fiber density.¹⁵ Morphological changes of the sub-basal nerve plexus, such as the beading, length, branching, and tortuosity of the nerve fiber, are related to the presence of SFN.^{11,16} There are several quantification methods available to analyze corneal nerve fibers¹⁷ ranging from manual analysis,¹⁸ semiautomatic analy-

sis,¹⁹ to automatic analysis.^{20,21} Parameters such as corneal nerve fiber density (CNFD), corneal nerve fiber length (CNFL), corneal nerve branch density (CNBD), and nerve fiber area (NFA) can be identified using these techniques. However, guidelines on which analysis system should be used are lacking, as well as data on comparison of these different programs.

CNFD counts the number of main nerves in the image (no./mm²), CNBD counts the number of branches (no./mm²), and CNFL counts the total length of both main nerves and branches (mm/mm²). Compared with CNFL, NFA is defined by the sum of total length of both main nerves and branches and the variation in the width ($\mu\text{m}^2/\text{mm}^2$) of nerve the fibers. As a result, NFA shows a nonlinear relation with CNFL and provides additional information when the structure but not the length of the small fibers changes. In the early stage of SFN, nerves tend to swell, whereas nerve degeneration can be observed in a more advanced stage of SFN. We illustrated this process in Figure 1, which was based on the study describing this nerve pathology.⁶ Based on the fact that, in the early phase of SFN development, NFL remains stable (Fig. 1), it is suggested that the use of NFA increases the sensitivity for diagnosing SFN.²¹ To date, no study has examined the correlation between NFA FIJI and ACCMetrics NFA. In patients with and without diabetes, there is good agreement between manual, semiautomatic, and automatic analyses of CNFL.²²

Looking at the different etiopathogeneses of diabetes and sarcoidosis, it remains to be seen whether the results found in patients with diabetes can be extrapolated to patients with sarcoidosis.²³ For example, it is known that patients with diabetes exhibit a more length-dependent variant of SFN, whereas SFN in patients with immune-mediated disease tends to present in a more patchy, non-length-dependent pattern.²⁴

The prevalence of ocular involvement in sarcoidosis ranges between 10-50%, with a higher prevalence reported in African Americans and women.²⁵ Ocular sarcoidosis could cause keratoconjunctivitis sicca, which then results in superficial punctate keratitis or band keratopathy, which in turn can affect the Bowman's epithelial layer.²⁶ In addition, uveitis can result in glaucoma, which can also contribute to decreased CNFD.²⁷

The aim of the current study was threefold. First, we investigated whether CCM results differ between patients with sarcoidosis with and without SFN. Secondly, we determined the correlation of CNFL calculated with manual analysis (CCMetrics¹⁸), semiautomatic analysis (NeuronJ¹⁹), and fully automatic analysis (ACCMetrics²⁰), and the correlation of NFA calculated with NFA FIJI²¹ and ACCMetrics in patients with sarcoidosis. Finally, the potential value of automatic NFA analysis in diagnosing SFN was evaluated.

Methods

Design

This was a prospective, cross-sectional observational study. Patients with sarcoidosis with and without clinical symptoms of SFN between 18 and 75 years of age were included between January 2021 and September 2022. In addition, colleagues and partners of patients with sarcoidosis were included as healthy controls. The diagnosis of sarcoidosis was made based on the official American Thoracic Society clinical practice guideline.¹ Exclusion criteria were established polyneuropathy, diseases associated with (poly)neuropathy, other diseases with a risk of developing (poly)neuropathy, neurological diseases affecting sensory nerve function, language difficulties, cognitive failure, glaucoma, corneal dystrophy, cornea infection, previous corneal surgery, contact lenses use, pregnancy, and excessive alcohol consumption.

Blood was tested for serum levels of glucose, creatine kinase (muscle damage), and vitamin B₁₂ in addition to all known parameters used to diagnose sarcoidosis. The study was conducted according to the

Declaration of Helsinki and Good Clinical Practice guidelines. All participants provided informed consent for study number R19.080 before the start of the analysis.

Ophthalmologic Assessment

The eye condition of participants was assessed by the ophthalmologist. General eye condition, glaucoma, keratoconus, and uveitis were evaluated based on visual acuity, best-corrected visual acuity, slit-lamp examination, and fundoscopy. The grade of the anterior chamber angle of the eye was determined using the Van Herrick technique.

Assessment of Neuropathy

A diagnosis of SFN was based on the Besta criteria,⁵ except for a skin biopsy. All participants underwent a detailed assessment of neuropathy by a neurologist. Participants were asked to report any type of annoying spontaneous or evoked pain sensations. Extensive neurological physical examination was used to test for clinical signs of SFN. Participants completed the SFN screening list (SFNSL)²⁸ to quantify somatic and autonomic symptoms. The SFNSL can be divided into two parts: part I (8 questions) assesses the frequency of complaints and part II (13 questions) assesses the severity of the complaints. The response scale ranged from 0 to 4 per item and a total number of 84 points was the maximum. An SFNSL of <11 was defined as no SFN, an SFNSL of 11 to 48 was defined as possible SFN, and an SFNSL of >48 was defined as definite SFN.²⁸

Sensory and motor nerve conduction studies were performed to exclude large fiber involvement. Surface recording electrodes with standard placement were used to measure compound muscle action potential, sensory nerve action potential, and nerve conduction. Motor nerve conduction was assessed for peroneal and tibial nerves and sensory nerve conduction was assessed for the sural nerve.

Quantitative Sensory Testing

QST measurements were performed on both feet. Cold and warm detection thresholds with the method of limits, thermal sensory limen, paroxysmal heat sensations, and cold and heat pain thresholds were performed according to the standard operating procedures described by the German Research Network on Neuropathic Pain.²⁹ Normative values published by the German Research Network on Neuropathic Pain group were used as cutoff values.³⁰ Patients with clinical signs, normal nerve conduction studies and at least

two QST abnormalities, were defined as established SFN.³¹

Corneal Confocal Microscopy

The Heidelberg Retinal Tomograph 3 with Rostock Corneal Module (Heidelberg Engineering GmbH, Dossenheim, Germany) was used to image the corneal sub-basal nerve plexus. A set up piece of +12 dpt. was used with an $\times 63$ objective lens. Using this set up, 384×384 pixels images of $400 \times 400 \mu\text{m}$ cornea tissue were generated. To obtain high-quality imaging, a widely available protocol³² for CCM imaging was used.

Analysis of Images

The software package CCMetrics was developed at the University of Manchester for manual analysis

of nerve tracing.¹⁸ Analysis was performed according to a standardized protocol.¹³ CCMetrics calculated the average CNFL from the selected images. CNFL was defined as the total length of all nerve fibers in the image (in units mm/mm^2).¹⁸ ACCMetrics was also developed at the University of Manchester for automatic nerve tracing analysis. It was based on the same tracing criteria as CCMetrics.²⁰ Although those programs could also calculate other parameters, NeuronJ was limited to calculating CNFL. Therefore, the other parameters were considered beyond the scope of this study, with the exception of the NFA calculated with ACCMetrics.

The semiautomatic nerve tracing software package NeuronJ, a freely available plug-in module for ImageJ (Biomedical Imaging Group, version 1.4.3), was developed at Erasmus Medical Center, Rotterdam, the Netherlands.¹⁹ Manual initiation at the beginning of

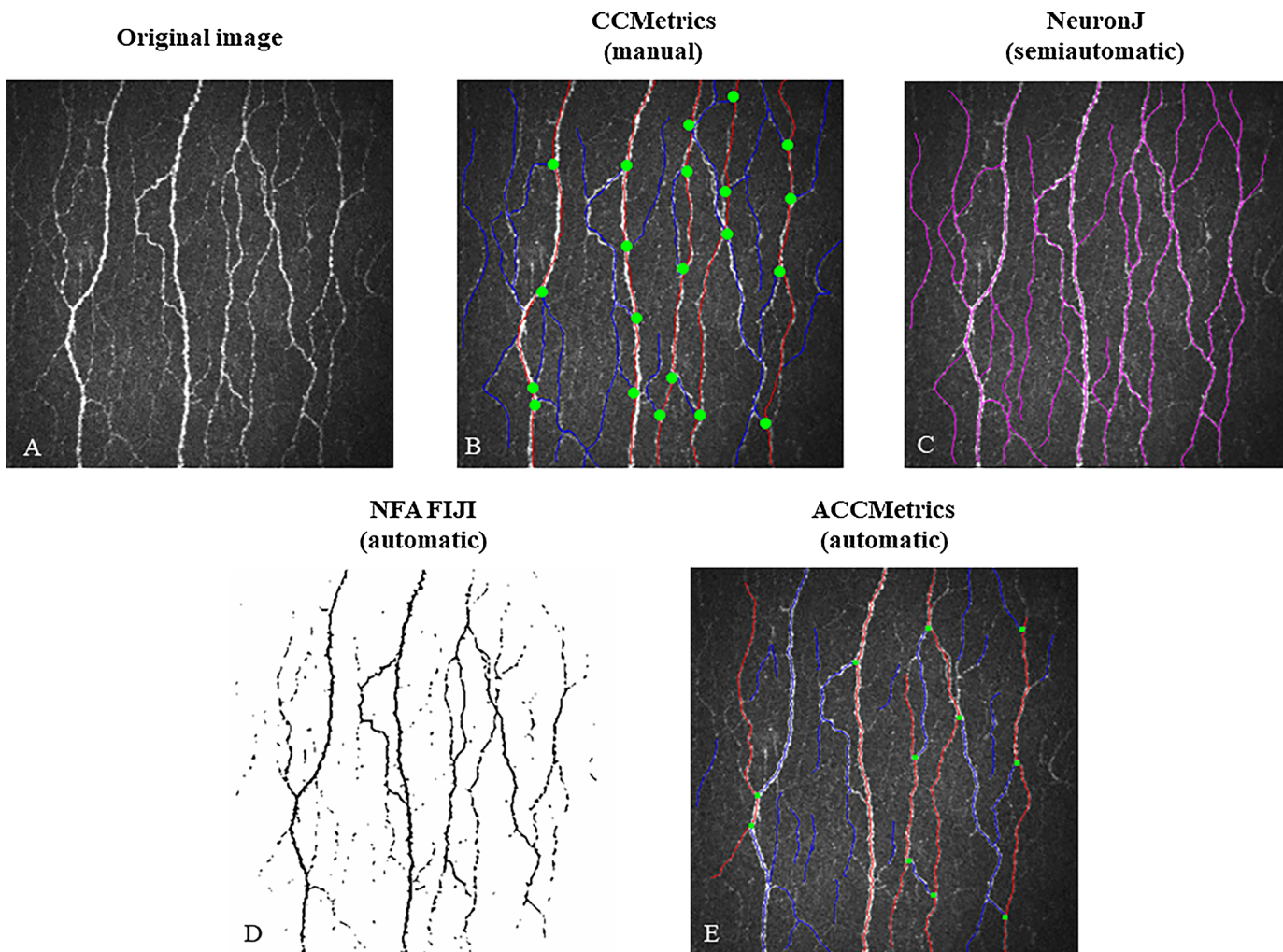


Figure 2. Examples of NFL calculations. (A) The original $400 \times 400 \mu\text{m}$ image of a patient with sarcoidosis and SFN symptoms. (B) Manual analysis performed with CCMetrics (CNFL = $25.8 \text{ mm}/\text{mm}^2$). (C) Semiautomatic analysis with NeuronJ (CNFL = $31.74 \text{ mm}/\text{mm}^2$). (D) Automatic analysis NFA FIJI (NFA = $19,650 \mu\text{m}^2/\text{mm}^2$). (E) Automatic analysis performed with ACCMetrics (CNFL = $20.46 \text{ mm}/\text{mm}^2$).

a nerve was required for nerve tracing; the algorithm then calculated the optimal tracing path. When low resolution of a nerve resulted in a failed tracing, manual corrections were possible. The number of highlighted pixels was the output of this program. Because the resolution and image size were known, simple math allowed converting the number of pixels to length in mm and vice versa.

NFA FIJI was a custom developed macro for FIJI.²¹ After several filtering steps described in the original paper³³; it quantifies the total number of pixels of a nerve plexus in an image. NFA is a two-dimensional metric that provides additional information about the full spectrum of variation in the nerve plexus. NFA FIJI results were compared with ACCMetrics NFA and with data from another study.²¹ This previous study defined a relationship between NFA FIJI and CNFL calculated with ACCMetrics. We reproduced that calculation; in addition, we defined a relationship between CCMetrics and NFA FIJI, as well as between NeuronJ and NFA FIJI. Because ACCMetrics, CCMetrics, and NeuronJ were expected to correlate, similar nonlinear relations with NFA FIJI were expected.

Three images from the center of the cornea of both eyes were used for manual (CCMetrics¹⁸) and semiautomatic (NeuronJ¹⁹) analysis. The selection was based on one image with a lower, one with a moderate, and one with a higher nerve fiber density for both eyes. The number of images was reduced for manual and semiautomatic analysis to maintain an acceptable workload. As a results, six images per individual were assessed. For automatic analysis (ACCMetrics²⁰ and NFA FIJI²¹), all good quality images were selected, because more measurements often result in more reliable results combined with a lower risk of selection bias.

An example of a representative image analysis is shown in Figure 2. The original image is shown in Figure 2A. CCMetrics (Fig. 2B) and NeuronJ (Fig. 2C) were affected by manual actions. NFA FIJI (Fig. 2D) was based on completely different algorithms and showed a skeletonized image. ACCMetrics analysis (Fig. 2E) is calculated completely automatically.

First, Kruskal–Wallis tests were applied to analyze differences in CNFL between four groups for the different software methods. Pearson's χ^2 logistic regression was then used to calculate correlation coefficients and 95% confidence interval for intraclass correlation coefficient. Bland–Altman plots were used to determine the agreement between the same parameter calculated with different software techniques. Finally, the quadratic relationship between CNFL and CNFA was

reproduced based on linear regression and the passing BabLock technique as described by Brines et al.²¹

Results

Patient Characteristics

Figure 3 shows an overview of the inclusion process. A total of 117 participants were included in this study. In 31 patients with sarcoidosis (26%), the diagnosis of established SFN was based on symptoms of SFN, clinical signs, normal nerve conduction studies, and at least two abnormal QST parameters of the feet.⁴ In 17 patients with sarcoidosis, symptoms, and clinical signs of SFN, no abnormalities in QST and/or SFNSL could be found (15%). Twenty-five patients with symptoms of SFN show no clinical signs of SFN and were, therefore, combined with patients without symptoms of SFN (42%) into the group patients with sarcoidosis without clinical signs of SFN. A total of 20 healthy controls were included and all met the inclusion criteria (17%).

Table 1 provides additional information on patient characteristics. The mean SFNSL score was significantly higher in patients with established SFN ($P < 0.001$). The SFNSL score was 44 in patients with sarcoidosis and established SFN, 35 in patients with sarcoidosis with probable SFN, 25 in patients with sarcoidosis without SFN, and 3 in healthy controls. The mean age of the patients was 52 ± 10 years and slightly more men were included (58%).

Cornea NFL in SFN

The mean CNFL and NFA for the four groups were calculated and ACCMetrics showed significantly higher CNFL and CNFA in patients with symptoms and clinical signs of SFN but with less than two abnormal thermal threshold testing parameters (see Table 2 and Fig. 4).

Correlation Between Programs

CCMetrics, NeuronJ, and ACCMetrics obtained values correlated well (correlation coefficient, 0.82–0.86; $P < 0.0001$), as did NFA FIJI and ACCMetrics NFA (correlation coefficient, 0.54; $P < 0.0001$). The strongest correlation existed between NeuronJ and CCMetrics ($R = 0.86$) (see Table 3). Furthermore, inter-rater agreement was excellent between CCMetrics, NeuronJ, and ACCMetrics and fair between NFA FIJI and ACCMetrics.

Bland–Altman plots comparing the manual analysis method with the semiautomatic and automatic

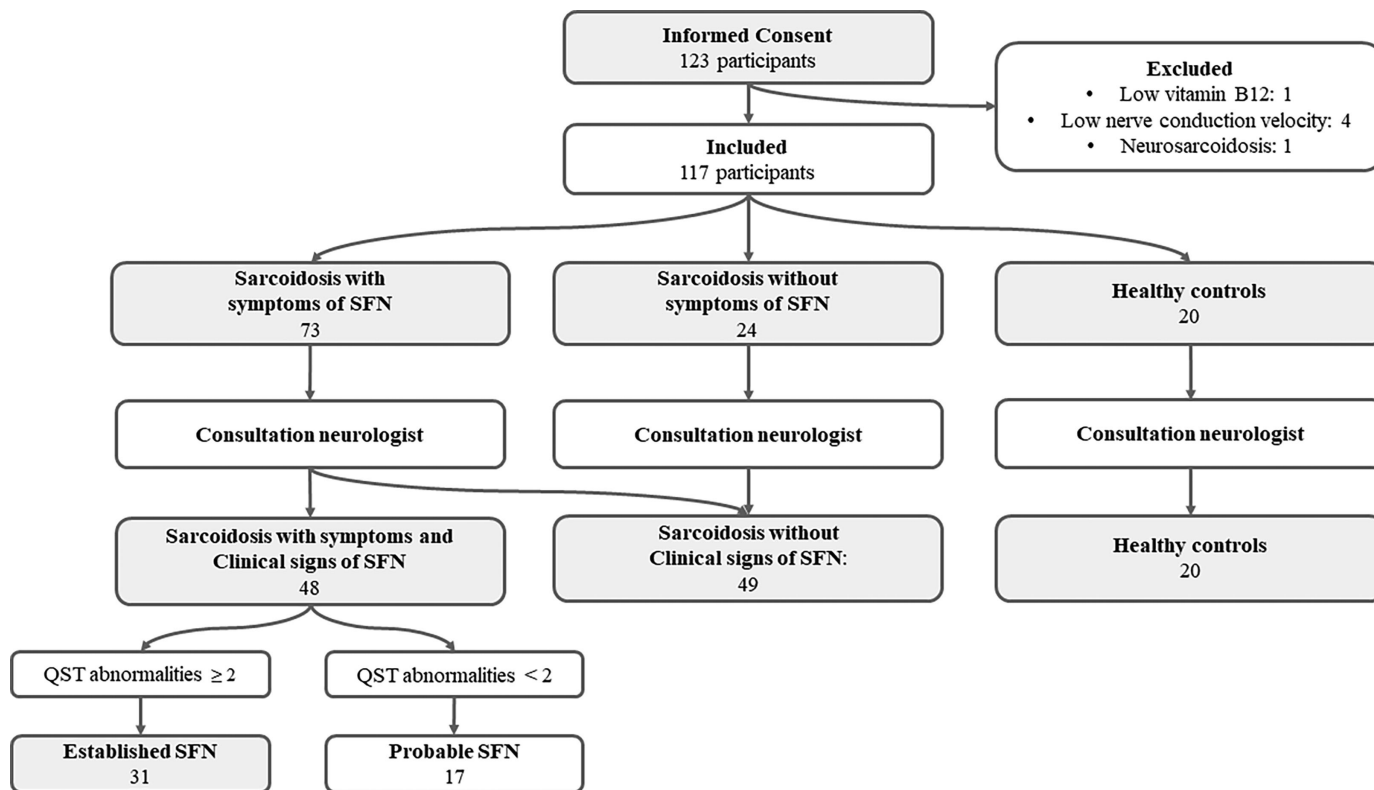


Figure 3. Inclusion and exclusion process; vitamin B₁₂ levels were decreased in one patient, nerve conduction velocity was decreased in four patients, one patient refused the visit owing to an impractical combination of eye drops during a working day, and one patient was diagnosed with neurosarcoidosis. In all, 117 participants were eligible for inclusion.

Table 1. Demographics in Patients With Sarcoidosis and Healthy Controls

Group	n	Age (Years)	Male Sex, n (%)	Height (cm)	BMI	Disease Duration Sarcoidosis (Years)	SFNSL
Healthy control	20	48 ± 12	10 (50%)	176 ± 9	23 ± 2		3 ± 4
Sarcoidosis without SFN	49	52 ± 11	36 (73%)	178 ± 9	26 ± 4	8 ± 6	25 ± 17
Sarcoidosis with probable SFN	17	50 ± 9	9 (29%)	176 ± 11	29 ± 6	7 ± 8	35 ± 10
Sarcoidosis with established SFN	31	52 ± 9	12 (39%)	176 ± 10	28 ± 6	9 ± 7	44 ± 11

analysis methods are shown in Figure 5, as well as the comparison of NFA FIJI and ACCMetrics NFA. The difference between CCMetrics and ACCMetrics showed a slight ascending slope (Fig. 5A), indicating that obtaining mean CNFL with CCMetrics resulted in slightly higher values compared with assessing CNFL with ACCMetrics. A nearly horizontal regression line was seen in the difference between CCMetrics and NeuronJ (Fig. 5B), suggesting similar results. There was a slight descending slope in the difference between ACCMetrics and NeuronJ (Fig. 5C), indicating that CNFL obtained with ACCMetrics showed slightly lower values than CNFL obtained with NeuronJ. Again, a nearly horizontal regression line can be seen in the differ-

ence between NFA FIJI and ACCMetrics (Fig. 5D). Similar slope directions were available in a previous study.²²

Relation Between CNFL and NFA

The relationship between CNFL and NFA was nonlinear and the slope increased progressively as nerve fiber density increased. A quadratic formula was calculated by Brines et al.²¹ to describe this relationship: $NFA\ FIJI = 2.78 \times 10^{-4} (NFL)^2 + 0.72 (NFL) + 471$. According to this exponential formula, NFA increased more than CNFL when the number of corneal nerve fibers increases. The formula was the result of linear regression analysis and the

Table 2. Mean CNFL and NFA Calculated With Different Analysis Methods

Analysis Method	Healthy Controls	No SFN	Probable SFN	Established SFN	P Value
CCMetrics (mm/mm ²)	14.7 ± 2.7	14.5 ± 4.5	15.7 ± 3.6	13.3 ± 4.1	0.6
NeuronJ (mm/mm ²)	17.5 ± 3.0	17.0 ± 4.1	18.6 ± 4.8	16.1 ± 4.2	0.8
ACCMetrics (mm/mm ²)	14.1 ± 2.6	13.2 ± 3.6	15.0 ± 4.7	12.1 ± 4.3	0.1
NFA FIJI (µm ² /mm ²)	5101.3 ± 1361.1	4879.2 ± 1408.3	6141.2 ± 1831.0	4781.8 ± 1888.2	0.01
ACCMetrics NFA (µm ² /mm ²)	4720.0 ± 787.8	4940.8 ± 1422.0	6141.2 ± 2379.1	4990.3 ± 1953.4	0.4

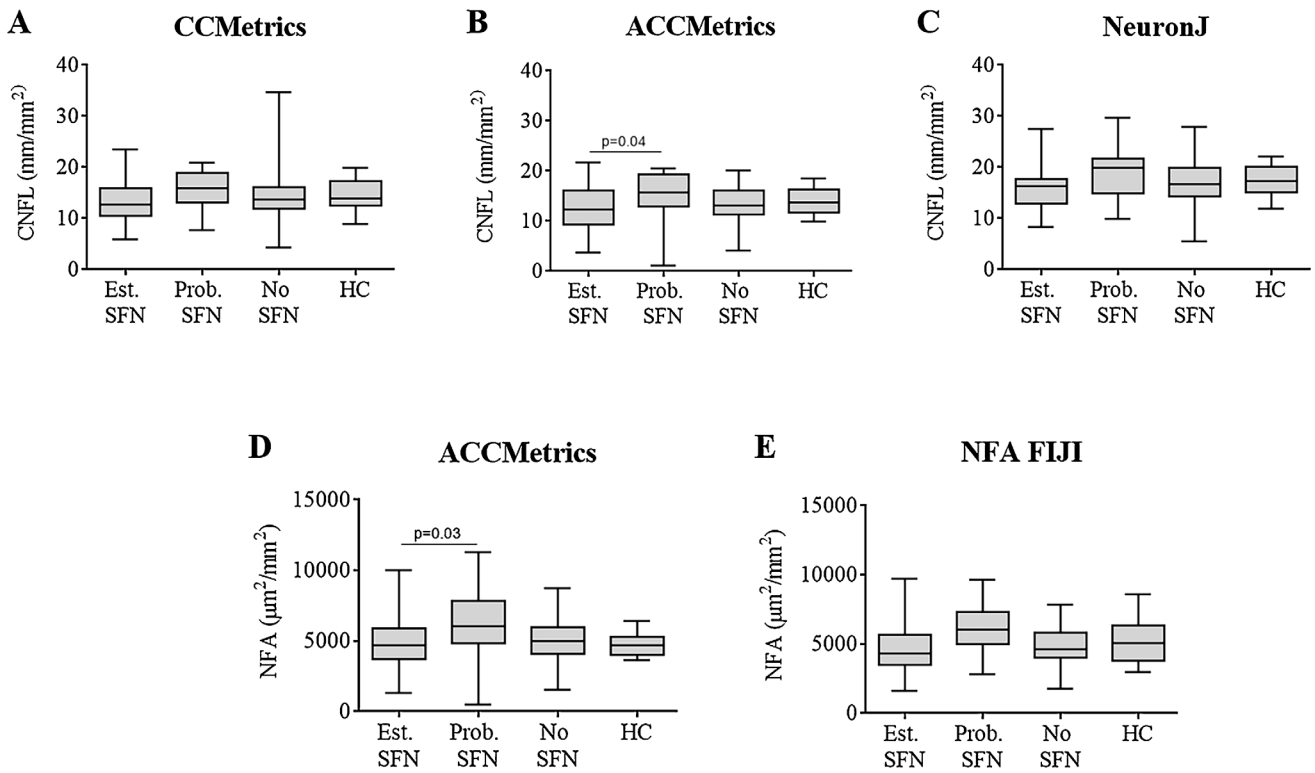


Figure 4. CNFL and cornea NFA (CNFA) boxplots, 25th to 75th percentiles, whiskers min to max and median lines. Four groups were defined based on established SFN, probable SFN, no SFN and healthy controls (HC). (A) CNFL measured with CCMetrics. (B) CNFL measured with ACCMetrics. (C) CNFL measured with NeuronJ. (D) NFA measured with NFA FIJI. (E) NFA measured with ACCMetrics. CNFL and NFA were unable to distinguish between patients with sarcoidosis with established SFN and without SFN.

Table 3. Correlation Between CCMetrics, ACCMetrics, NeuronJ, and NFA FIJI

Analysis Systems	R Value	P Value	ICC 95% Confidence Interval
CCMetrics vs. ACCMetrics	0.82	<0.0001	0.75–0.87
CCMetrics vs. NeuronJ	0.86	<0.0001	0.80–0.90
ACCMetrics vs. NeuronJ	0.82	<0.0001	0.74–0.87
NFA FIJI vs. ACCMetrics NFA	0.54	<0.0001	0.39–0.66

use of passing BabLock technique. Figure 6 shows the formula from Brines et al.²¹ compared with our data in patients with sarcoidosis. When calculating our own formula with the same technique and programs (ACCMetrics CNFL and NFA FIJI), the line was

somewhat shifted to higher values, following approximately the same progression (Fig. 6A). However, for CCMetrics and NeuronJ, a root curve (blue) described the relationship instead of exponential growth. As a result, the increase in NFA would decrease as the

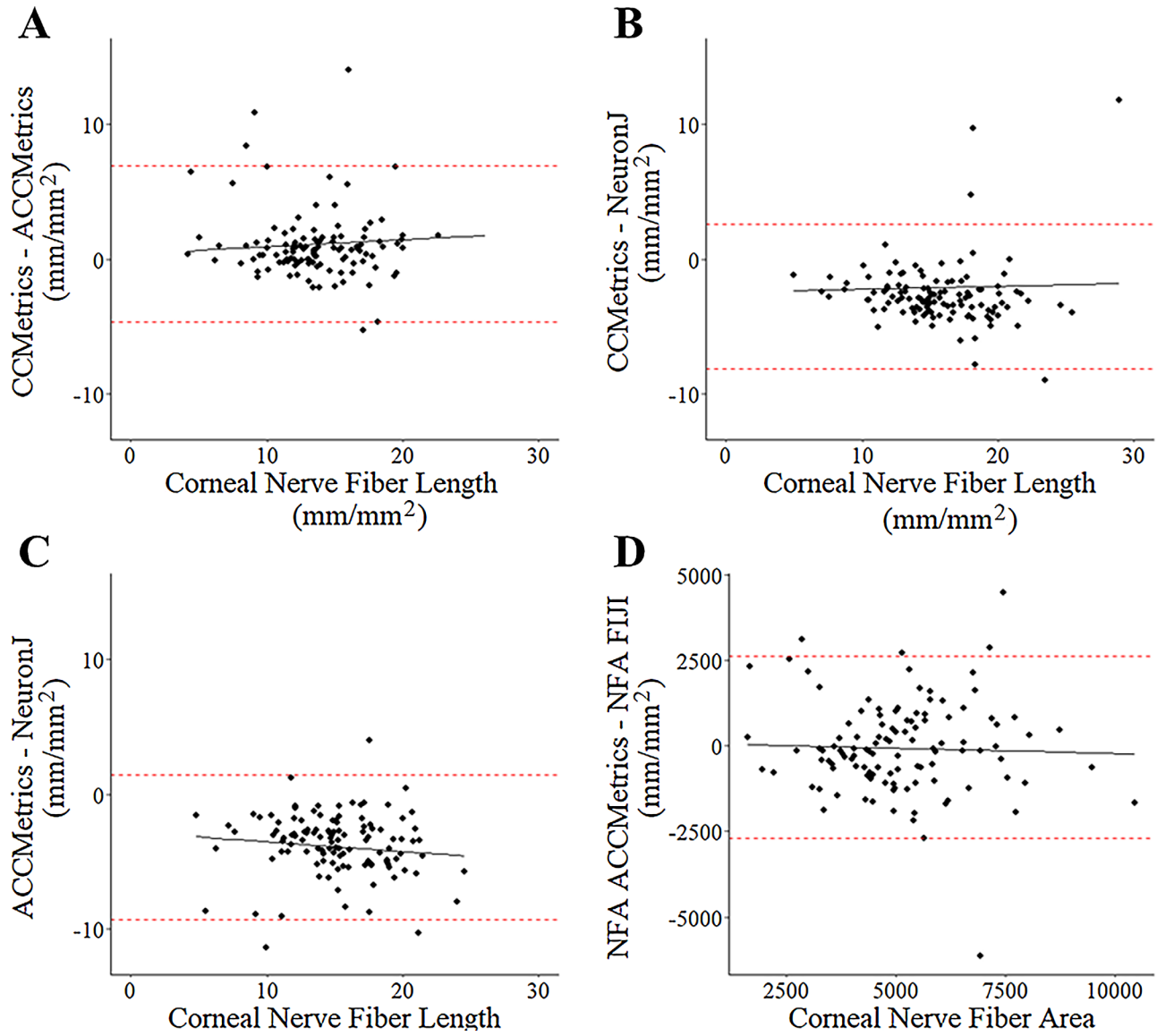


Figure 5. Bland–Altman plots between (A) CCMetrics and ACCMetrics, (B) CCMetrics and NeuronJ, (C) ACCMetrics and NeuronJ, and (D) ACCMetrics and NFA FIJI.

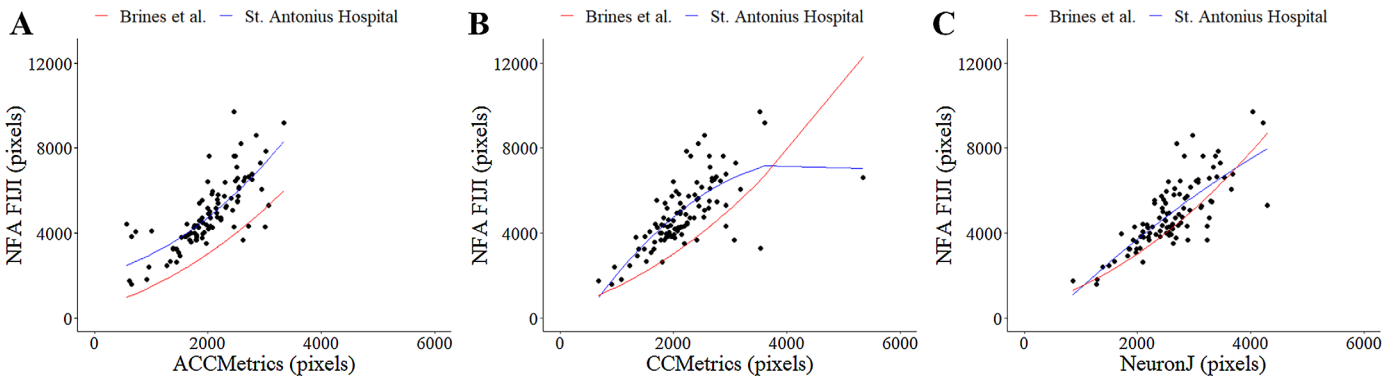


Figure 6. Second-order polynomial regression plot to calculate the relationship between cornea NFA and CNFL. The formula of Brines et al. was compared with the formula calculated with data from this study. (A) CCMetrics and NFA FIJI, described by $NFA = -4.66 \times 10^{-4} (CNFL)^2 + 4.1 (CNFL) - 1580$. (B) ACCMetrics and NFA FIJI, described by $NFA = 3.94 \times 10^{-4} (CNFL)^2 + 5.57 \times 10^{-1} (CNFL) + 2041$. (C) NeuronJ and NFA FIJI, described by $NFA = -1.33 \times 10^{-4} (CNFL)^2 + 2.68(CNFL) - 1123$.

number of corneal nerve fibers increases (Figs. 6B and 6C).

Discussion

In the present study, we did not demonstrate reduced CNFL and NFA in patients with sarcoidosis with and without established SFN compared with healthy controls (see Fig. 4). Multiple analytical methods to determine CNFD show a strong correlation. Automatic analysis showed similar results with manual or semiautomatic methods (see Table 3 and Fig. 5). NFA calculated with NFA FIJI was comparable with ACCMetrics, but showed a lower 95% confidence interval. Moreover, a nonlinear relationship between NFA and CNFL could be confirmed (see Fig. 6).

When interpreting CCM results, the consequences of ocular sarcoidosis affecting the cornea should be taken into account. To rule out bias from sarcoidosis or other causes of reduced CNFL rather than pure SFN, eye condition was examined in all participants. Therefore, participants with glaucoma, corneal dystrophy, corneal infection, previous corneal surgery, and contact lens use were excluded from this study.

Unexpectedly, CNFL and CNFA were not reduced in patients with sarcoidosis and established SFN compared with patients with sarcoidosis without SFN or healthy controls. Figure 1 shows the course of small nerve fibers during nerve damage. In severe SFN, regeneration of small nerve fibers occurs as a result of sprouting. Regenerated nerves exhibit higher tortuosity. It could be possible that tortuous nerves show higher CNFL in the same area of $400\ \mu\text{m}^2$ compared with less tortuous nerves, which could compensate for the decrease of CNFL. Furthermore, sprouting could lead to hyper-reinnervation, resulting in higher CNFL.³⁴ It is unclear which phases of nerve damage are present in persistent SFN. There are no studies available for patients with sarcoidosis with SFN that clearly describe the course of persistent SFN. Therefore, it is currently unclear whether persistent SFN is progressive or whether different phases of nerve damage and sprouting present simultaneously.

ACCMetrics demonstrated higher CNFL and CNFA in patients with sarcoidosis with symptoms and clinical signs of SFN and fewer than two thermal threshold testing parameters compared with patients with established SFN. As shown in Figure 1, increased CNFA can be explained by nerve swelling and increased CNFL can be explained by increased nerve tortuosity. However, these phenomena occur in differ-

ent phases; therefore, it seems unlikely that they are the reason for these results, which are present simultaneously. No clear explanation could be found as to why patients with probable SFN showed increased CNFL and CNFA compared with patients with established SFN.

To our knowledge, few studies have compared CNFL results, but none compared NFA FIJI results with NFA calculated with ACCMetrics or results of NFA FIJI with CNFL values from manual methods. Our study confirmed a good correlation between manual analysis (CCMetrics¹⁸), semiautomatic analysis (NeuronJ¹⁹), and fully automatic analysis (ACCMetrics²⁰) in a cohort of patients with sarcoidosis, as well as NFA FIJI and ACCMetrics calculated NFA. To improve the clinical applicability of CCM, automatic imaging analysis is preferred. Although normative values for corneal nerve parameters are established using manual analysis methods,¹² clinical applicability would greatly benefit from an automatic approach. Our results showed that an automatic approach is indeed feasible, that the results of automatic analysis are similar to the results of manual methods, and that different automatic techniques are sufficiently correlated to allow direct comparison of results obtained with different methods.

Although a good correlation was demonstrated, some minor details regarding the differences between the analysis techniques should be discussed. First, there may be a selection bias between manual, semiautomatic, and automatic analysis techniques. For manual and semiautomatic analysis, only six images were selected for analysis, whereas for automatic methods, all images of good quality were selected. Manual analysis methods required selecting a limited number of images to maintain an acceptable workload. However, selecting all images of good quality would decrease the risk of selection bias if future protocols include automatic analysis. Furthermore, this approach is suitable for automatic analysis because increasing the number of images does not increase workload. To make a good comparison between the different analysis programs, these differences in methods have already been taken into account.

Second, the automatic analysis technique was prone to a small underestimation of CNFL compared with the manual and semiautomatic analysis techniques (Fig. 5). This practice is consistent with previous research²² that examined the same software programs. As discussed in the previous article, this factor can probably be explained by the human eye's ability to detect more complicated lines as nerve fibers, whereas the automatic system was limited by strict criteria. Furthermore, the fully automatic analysis generated

both false-positive and false-negative errors. Thin nerves and nerves out of focus were prone to false-negative errors, and other structures such as dendritic cells were prone to false-positive errors.

Third, a small difference was the slightly higher values obtained with NeuronJ compared with CCMetrics. As mentioned elsewhere in this article, CCMetrics calculated values by manual nerve tracing, whereas NeuronJ traced the nerves semiautomatically. An automatic algorithm calculated the optimal nerve path, guided by manual instructions. Therefore, manual instructions were only necessary when the algorithm had a tendency to choose a wrong path. Compared with CCMetrics, this method was much faster and drew lines more easily than the fully manual method. This method, therefore, resulted in slightly higher values compared with CCMetrics.

Finally, although NFA FIJI and ACCMetrics NFA showed a highly significant correlation, they also showed the lowest inter-rater agreement. The only difference discovered between NFA FIJI and ACCMetrics NFA was that ACCMetrics calculates NFA in mm^2/mm^2 , whereas NFA FIJI calculates in $\mu\text{m}^2/\text{mm}^2$. The lowest step size for ACCMetrics was $100 \mu\text{m}^2/\text{mm}^2$, whereas NFA FIJI was more accurate up to single $\mu\text{m}^2/\text{mm}^2$. However, this factor does not necessarily lead to lower inter-rater agreement.

A previous study²¹ was able to distinguish between patients with sarcoidosis and diabetes with NFA in a higher CNFL range ($>9.8 \text{ mm}/\text{mm}^2$). Patients with sarcoidosis showed lower NFA compared with patients with diabetes. For the same group, CNFL was not significantly different between patients with sarcoidosis and diabetes. Therefore, they concluded that NFA reveals additional information as a function of neuropathic severity. However, it remained unknown whether NFA could differentiate neuropathic severity within a group of patients with sarcoidosis. However, as shown in Figure 6, our data showed that patients with sarcoidosis with and without SFN have no difference in NFA measured by CCM. Therefore, our study does not support the potential value of NFA in the diagnosis of SFN in patients with sarcoidosis. One explanation could be that the nerve fiber width is significantly greater in subjects with sarcoidosis compared with diabetic patients and healthy subjects.²¹ However, healthy controls showed the same NFA compared with both sarcoidosis groups. Therefore, we believe that NFA cannot be used as a diagnostic criterion for distinguishing patients with sarcoidosis with and without SFN.

Previous research described the relationship between CNFL and NFA using an exponential formula. We reproduced this formula based on our

own data and compared it with the formula from the other study. With CNFL measured by ACCMetrics, a similar relationship could be described with a shift toward higher values. Compared with the previous study,²¹ sarcoidosis measurements from our study were limited to the central part of their curve. In addition, the previous study included subjects with diabetic (distributed in the left lower part of the curve) and healthy subjects (distributed in the right upper part). The lack of diabetic patients in our dataset could partially explain the shift in our curve. Moreover, the fact that patients with sarcoidosis already showed wider nerve fibers could also be another.²¹

The relationship between CNFL and NFA, described by the formulas based on CCMetrics and NeuronJ, unexpectedly showed a root relationship instead of an exponential relationship. Therefore, the previously provided formula was not generally applicable to any software program with CNFL as output. This finding could not be explained by physiological causes because the same population was used. As a result, this finding must be explained by technical differences. Despite the excellent correlation between the methods, a combination of selection bias and a small underestimation of the automatic analysis was thought to be responsible for distorting a fair comparison.

Limitations of these methods were that only CNFL and NFA could be compared using different analysis systems and that CNFL was sometimes underestimated. CNFD and CNBD were not calculated with NeuronJ and, therefore, could not be compared with the other analysis methods. Defining the density and branches required more complicated algorithms. The other limitation was that CNFL may have been underestimated if the quality of the images was not optimal. The outer edges of CCM images were sometimes blurred, which directly affected the CNFL. In addition, pressure lines sometimes interrupted the nerves when the patient's cornea was difficult to photograph, although this difficulty was avoided as much as possible. This factor could result in a lower CNFL. To attenuate this limitation, reduced CNFL was observed in a minority of 35% of participants and equally distributed across the three groups. Therefore, the effect of image quality on the results of this study was estimated as limited. For future studies, implementing a quality index could add value to identifying the effects of image quality.³⁵

Strengths of this study were the unique study population and new insights regarding the added value of NFA compared with multiple image analysis techniques. This study included a large group of patients with the rare diseases sarcoidosis and SFN,

whereas the majority of research with CCM to date has been applied on patients with diabetes. Because sarcoidosis is a very complicated disease with heterogeneous presentations, it was important to investigate whether current CCM methods were applicable to this group. Furthermore, no study has previously directly compared these four analysis methods. This study clearly identified the relation between different image analysis techniques and helped to elucidate the origin of the differences between these systems. Discrimination between SFN and no SFN could not be achieved in this study population based on CNFL or NFA.

In conclusion, although no strong decrease of CNFL could be found in patients with sarcoidosis, automatic analysis could be used to reduce workload for imaging analysis. Furthermore, the theory that nerve fiber morphology changes before degeneration and could be measured with NFA did not seem useful to distinguish between patients with sarcoidosis with and without SFN. Further research is needed to understand the exact morphological changes of small nerve fibers in different diseases. Furthermore, determining normative values for NFA would help to identify different phases of SFN when measured in combination with other corneal nerve parameters.

Acknowledgments

Funding provided by ZonMW TopZorg 842002001.

Disclosure: **L.R.M. Raasing**, None; **O.J.M. Vogels**, None; **M. Datema**, None; **M.R. Tannemaat**, None; **M. Veltkamp**, None; **J.C. Grutters**, None

References

1. Crouser ED, Maier LA, Baughman RP, et al. Diagnosis and detection of sarcoidosis: an official American Thoracic Society Clinical practice guideline. *Am J Respir Crit Care Med*. 2020;201:E26–E51, doi:10.1164/RCCM.202002-0251ST.
2. Tavee J. Peripheral neuropathy in sarcoidosis. *J Neuroimmunol*. 2022;368:577864, doi:10.1016/j.jneuroim.2022.577864.
3. Voortman M, Hendriks CMR, Elfferich MDP, et al. The burden of sarcoidosis symptoms from a patient perspective. *Lung*. 2019;197:155–161, doi:10.1007/s00408-019-00206-7.
4. Tesfaye S, Boulton AJM, Dyck PJ, et al. Diabetic neuropathies: update on definitions, diagnostic criteria, estimation of severity, and treatments. *Diabetes Care*. 2010;33:2285–2293, doi:10.2337/dc10-1303.
5. Devigili G, Rinaldo S, Lombardi R, et al. Diagnostic criteria for small fibre neuropathy in clinical practice and research. *Brain*. 2019;142:3728–3736, doi:10.1093/brain/awz333.
6. Lauria G, Morbin M, Lombardi R, et al. Axonal swellings predict the degeneration of epidermal nerve fibers in painful neuropathies. *Neurology*. 2003;61:631–636, doi:10.1212/01.WNL.0000070781.92512.A4.
7. Lauria G, Bakkens M, Schmitz C, et al. Intraepidermal nerve fiber density at the distal leg: a worldwide normative reference study. *J Peripher Nerv Syst*. 2010;15:202–207, doi:10.1111/j.1529-8027.2010.00271.x.
8. Hansson P, Backonja M, Bouhassira D. Usefulness and limitations of quantitative sensory testing: clinical and research application in neuropathic pain states. *Pain*. 2007;129:256–259, doi:10.1016/j.pain.2007.03.030.
9. Quattrini C, Tavakoli M, Jeziorska M, et al. Surrogate markers of small fiber damage in human diabetic neuropathy. *Diabetes*. 2007;56:2148–2154, doi:10.2337/db07-0285.CCM.
10. Tavakoli M, Marshall A, Thompson L, et al. Corneal confocal microscopy: a novel noninvasive means to diagnose neuropathy in patients with Fabry disease. *Muscle Nerve*. 2009;40:976–984, doi:10.1002/mus.21383.
11. Oliveira-Soto L, Efron N. Morphology of corneal nerves using confocal microscopy. *Cornea*. 2001;20:374–384, doi:10.1097/00003226-200105000-00008.
12. Tavakoli M, Ferdousi M, Petropoulos IN, et al. Normative values for corneal nerve morphology assessed using corneal confocal microscopy: a multinational normative data set. *Diabetes Care*. 2015;38:838–843, doi:10.2337/dc14-2311.
13. Tavakoli M, Malik RA. Corneal confocal microscopy: a novel non-invasive technique to quantify small fibre pathology in peripheral neuropathies. *J Vis Exp*. 2011;3:2194, <http://www.embase.com/search/results?subaction=viewrecord&from=export&id=L560076652>.
14. Petropoulos IN, Ponirakis G, Khan A, et al. Corneal confocal microscopy: ready for prime time. *Clin Exp Optom*. 2019;103:265–277, doi:10.1111/cxo.12887.
15. Müller LJ, Vrensen GFJM, Pels L, Cardozo BN, Willekens B. Architecture of human corneal nerves. *Investig Ophthalmol Vis Sci*. 1997;38:985–994.

16. Malik RA, Kallinikos P, Abbott CA, et al. Corneal confocal microscopy: a non-invasive surrogate of nerve fibre damage and repair in diabetic patients. *Diabetologia*. 2003;46:683–688, doi:10.1007/s00125-003-1086-8.
17. Kim J, Markoulli M. Automatic analysis of corneal nerves imaged using in vivo confocal microscopy. *Clin Exp Optom*. 2018;101:147–161, doi:10.1111/cxo.12640.
18. Dabbah M, Graham J, Tavakoli M, et al. Nerve fibre extraction in confocal corneal microscopy images for human diabetic neuropathy detection using gabor filters. In: Dehmeshki J, Hoppe A, Greenhill D, eds. *Medical Image Understanding and Analysis: Proceedings of the Thirteenth Annual Conference*. Kingston University, UK: BMVA; 2009:254–258.
19. Meijering E, Jacob M, Sarria JCF, Steiner P, Hirling H, Unser M. Design and validation of a tool for neurite tracing and analysis in fluorescence microscopy images. *Cytometry*. 2004;58:167–176, doi:10.5040/9781474229050.0007.
20. Dabbah MA, Graham J, Petropoulos IN, Tavakoli M, Malik RA. Automatic analysis of diabetic peripheral neuropathy using multi-scale quantitative morphology of nerve fibres in corneal confocal microscopy imaging. *Med Image Anal*. 2011;15:738–747, doi:10.1016/j.media.2011.05.016.
21. Brines M, Culver DA, Ferdousi M, et al. Corneal nerve fiber size adds utility to the diagnosis and assessment of therapeutic response in patients with small fiber neuropathy. *Sci Rep*. 2018;8:1–11, doi:10.1038/s41598-018-23107-w.
22. Dehghani C, Pritchard N, Edwards K, Russell AW, Malik RA, Efron N. Fully automated, semiautomated, and manual morphometric analysis of corneal subbasal nerve plexus in individuals with and without diabetes. *Cornea*. 2014;33:696–702, doi:10.1097/ICO.000000000000152.
23. de Greef BTA, Hoesjmakers JGJ, Gorissen-Brouwers CML, Geerts M, Faber CG, Merkies ISJ. Associated conditions in small fiber neuropathy – a large cohort study and review of the literature. *Eur J Neurol*. 2018;25:348–355, doi:10.1111/ene.13508.
24. Khan S, Lan Z. Characterization of non-length-dependent small-fiber sensory neuropathy. *Muscle and Nerve*. 2012;45:86–91, doi:10.1002/mus.22255.
25. Sève P, Pacheco Y, Durupt F, et al. Sarcoidosis: a clinical overview from symptoms to diagnosis. *Cells*. 2021;10:766, doi:10.3390/cells10040766.
26. Pasadhika S, Rosenbaum JT. Ocular sarcoidosis. *Clin Chest Med*. 2015;36(4):669–683, <https://doi.org/10.1016/j.ccm.2015.08.009>.
27. Gatzioufas Z, Labiris G, Hafezi F, et al. Corneal sensitivity and morphology of the corneal subbasal nerve plexus in primary congenital glaucoma. *Eye*. 2014;28:466–471, doi:10.1038/eye.2014.4.
28. Hoitsma E, De Vries J, Drent M. The small fiber neuropathy screening list: construction and cross-validation in sarcoidosis. *Respir Med*. 2011;105:95–100, doi:10.1016/j.rmed.2010.09.014.
29. Rolke R, Andrews K, Magerl W, Treede RD. Quantitative sensory testing - investigator's brochure. *J Clin Neurophysiol*. 2010;12:192–202, doi:10.1097/00004691-199503000-00010.
30. Rolke R, Baron R, Maier C, et al. Quantitative sensory testing in the German Research Network on Neuropathic Pain (DFNS): standardized protocol and reference values. *Pain*. 2006;123:231–243, doi:10.1016/j.pain.2006.01.041.
31. Raasing LRM, Veltkamp M, Datema M, Grutters JC, Vogels OJM. Thermal threshold testing: call for a balance between the number of measurements and abnormalities in the diagnosis of sarcoidosis associated small fiber neuropathy. *Pain Reports*. 2023;8:e1095, doi:10.1097/PR9.000000000000109.
32. Tavakoli M, Malik RA. Corneal confocal microscopy: a novel non-invasive technique to quantify small fibre pathology in peripheral neuropathies. *J Vis Exp*. 2010;33:1792–1797, doi:10.3791/2194.
33. Chen X, Graham J, Petropoulos IN, et al. Corneal nerve fractal dimension: a novel corneal nerve metric for the diagnosis of diabetic sensorimotor polyneuropathy. *Investig Ophthalmol Vis Sci*. 2018;59:1113–1118, doi:10.1167/iovs.17-23342.
34. Marfurt CF, Ellis LC, Jones MA. Sensory and sympathetic nerve sprouting in the rat cornea following neonatal administration of capsaicin. *Somatosens Mot Res*. 1993;10:377–398, doi:10.3109/08990229309028845.
35. Sturm D, Vollert J, Greiner T, et al. Implementation of a quality index for improvement of quantification of corneal nerves in corneal confocal microscopy images. *Cornea*. 2019;38:1, doi:10.1097/ico.0000000000001949.